1521-0111/12/8106-770–777$25.00
MOLECULAR PHARMACOLOGY
Copyright © 2012 The American Society for Pharmacology and Experimental Therapeutics
Mol Pharmacol 81:770–777, 2012

Vol. 81, No. 6
77693/3768494

Nonequilibrium Activation of a G-Protein-Coupled Receptor

Manuela Ambrosio and Martin J. Lohse

Institute of Pharmacology and Toxicology, University of Würzburg, Würzburg, Germany

Received January 10, 2012; accepted February 29, 2012

ABSTRACT

G-protein-coupled receptor activation is generally analyzed under equilibrium conditions. However, real-life receptor functions are often dependent on very short, transient stimuli that may not allow the achievement of a steady state. This is particularly true for synaptic receptors such as the α_{2A}-adrenergic receptor (α_{2A}-AR). Therefore, we developed a fluorescence resonance energy transfer-based technology to study nonequilibrium α_{2A}-AR function in living cells. To examine the effects of increasing concentrations of the endogenous agonist norepinephrine on the speed and extent of α_{2A}-AR activation with very high temporal resolution, we took advantage of a fluorophore-containing α_{2A}-AR sensor. The results indicated that the efficacy of norepinephrine in eliciting receptor activation increased in a time-dependent way, reaching the maximum with a half-life of ~60 ms. The EC_{50} values under nonequilibrium conditions start at ~26 μM (at 40 ms) and show a 10-fold decrease until the steady state is achieved. To analyze the ability of norepinephrine to trigger a downstream intracellular response after α_{2A}-AR stimulation, we monitored the kinetics and amplitude of G_i activation in real time by using a fluorophore-containing G_i sensor. The results show that both the efficacy and the potency of norepinephrine in inducing G_i activation achieve a steady state more slowly, compared with receptor activation, and that the initial EC_{50} value of ~100 nM decreases in an exponential way, reaching the minimal value of ~10 nM at equilibrium. Therefore, both the efficacy and the potency of norepinephrine increase ~10-fold over a few seconds of agonist stimulation, which illustrates that receptor and G-protein signaling and signal amplification are highly time-dependent phenomena.

Introduction

G-protein-coupled receptors (GPCRs) represent the largest family of membrane receptors for a large number of diverse endogenous ligands, including hormones and neurotransmitters (Lefkowitz, 2000). The binding of an extracellular agonist to its receptor represents the initial step in the signaling pathway and has typically been investigated through radioligand binding experiments. Such studies allow the determination of equilibrium affinities (K_i and K_d values) and also yield important details about ligand association/dissociation rates at the receptor level (Hulme and Trevethick, 2010). However, such experiments require long incubation times (from several minutes to hours) and thus cannot represent a real-time approach. Furthermore, binding studies are limited to the interactions between ligands and receptors and cannot explore the activation of a receptor once it is bound to an agonist. After the binding of an extracellular agonist to its GPCR, the signaling pathway proceeds with the receptor switching from a resting state into an active conformation that allows the binding and activation of the cognate G-proteins and, hence, the transduction of a transmembrane signal to the downstream effectors (e.g., adenylyl cyclases, phospholipases, or ion channels). Because the agonist-induced receptor conformational rearrangements were not directly accessible until recently, GPCR activation was inferred traditionally from the stimulation of a receptor-mediated downstream biological response that could be easily measured experimentally. Together with binding assays, such activation assays led to the classic concepts of receptor theory. Most methods applied for these studies do not use intact cells and are usually performed under equilibrium conditions necessitating extended incubation times, which do not allow continuous, real-time monitoring of receptor activity. Under physiological conditions, however, receptor binding and activation often are dependent on very short stimuli and usually do not reach a steady state. This is especially true for receptors involved in synaptic transmission, such as α_{2A}-adrenergic receptors (α_{2A}-ARs). These rhodopsin-like GPCRs mediate the biological effects of endogenous catecholamines, most notably in presynaptic control of neurotransmitter release, thus playing a key role in the modulation of many physiological functions of the sympathetic nervous system (Philipp and Hein, 2004; Hein,

This work was supported by the Deutsche Forschungsgemeinschaft [Grant SFB487] and the European Research Council [Advanced Grant "Topas"].

Article, publication date, and citation information can be found at http://molpharm.aspetjournals.org.

http://dx.doi.org/10.1124/mol.112.077693.

ABBREVIATIONS: GPCR, G-protein-coupled receptor; α_{2A}-AR, α_{2A}-adrenergic receptor; FRET, fluorescence resonance energy transfer; FlAsH, fluorescein arsenical hairpin binder; YFP, yellow fluorescent protein; CFP, cyan fluorescent protein; HEK, human embryonic kidney; HBSS, Hanks' balanced salt solution.

2006). Norepinephrine is the principal neurotransmitter of postganglionic sympathetic nerves. Once released, it diffuses across the synaptic space and exerts its function by binding to and activating either presynaptic α_{2A}-ARs on the nerve ending or postsynaptic α_{2A}-ARs on the effector organ. Fast cyclic voltammetry measurements in multiple brain regions have shown that the maximal evoked norepinephrine release in vivo is in the micromolar range and that the time required for the overflow to decay to half of the maximum is a few seconds (Park et al., 2009, 2011).

Because the physiological dynamics of norepinephrine are not compatible with the classic approaches applied to detect receptor activation, we developed a technology to study nonequilibrium α_{2A}-AR function in real time. The development of optical techniques that permit the study of GPCR-mediated signaling processes in intact cells facilitates the analysis of distinct signaling steps in a more-physiological setting (reviewed by Lohse et al., 2008b). By taking advantage of a fluorescence resonance energy transfer (FRET)-based approach, it is possible to follow the conformational changes of GPCRs in living cells and to gain information about the characteristics and kinetics of GPCR activation in real time (Vilardaga et al., 2003). Placement of a donor fluorophore [e.g., cyan fluorescent protein (CFP)] and an acceptor fluorophore [e.g., small fluorescein arsenical hairpin binder (FlAsH)] in the third intracellular loop and at the C terminus, respectively, led to the development of an α_{2A}-AR sensor (Fig. 1) whose activation can be measured through intramolecular FRET recording. Kinetic measurements suggested previously that, given enough receptors and G-proteins, the receptor–G-protein interaction occurs as fast as receptor activation itself and therefore does not represent a time-limiting step in the signaling pathway (Hein et al., 2005, 2006). In contrast, the subsequent G-protein activation limits the progression of the receptor-mediated signaling cascade (Bünemann et al., 2003; Hein et al., 2006; Jensen et al., 2009); although receptor–G-protein interactions are already maximal after ~50 ms, only a small fraction of G-proteins are activated at that point, and it takes ~1 to 2 s until G-protein activation reaches its maximum.

These new techniques allow the study of receptor activation and signaling and thus the investigation of potencies and efficacies under nonequilibrium conditions. Here, taking advantage of both receptor and G-protein FRET-based sensors, we analyzed norepinephrine-induced α_{2A}-AR activation under nonequilibrium conditions. This approach allowed the real-time monitoring of norepinephrine-mediated effects occurring on a millisecond time scale in living cells, which reflect physiological synaptic events.

Materials and Methods

Materials. Norepinephrine was obtained from Sigma-Aldrich (St. Louis, MO). FlAsH is commercially available from Invitrogen (Carlsbad, CA) as TC-FlAsH.

Cell Culture and Transfection. Cells were seeded on round, polylysine-coated coverslips, which were placed in six-well plates and maintained in Dulbecco's modified Eagle's medium supplemented with 10% fetal calf serum, 10^5 U/liter penicillin, and 100 mg/liter streptomycin, at 37°C in 7% CO_2. HEK-293 cells stably expressing α_{2A}-AR$^{FlAsH/CFP}$ (Hoffmann et al., 2005) were described previously (Nikolaev et al., 2006). HEK-293 cells were transfected with plasmids encoding the wild-type α_{2A}-AR and the heterotrimeric

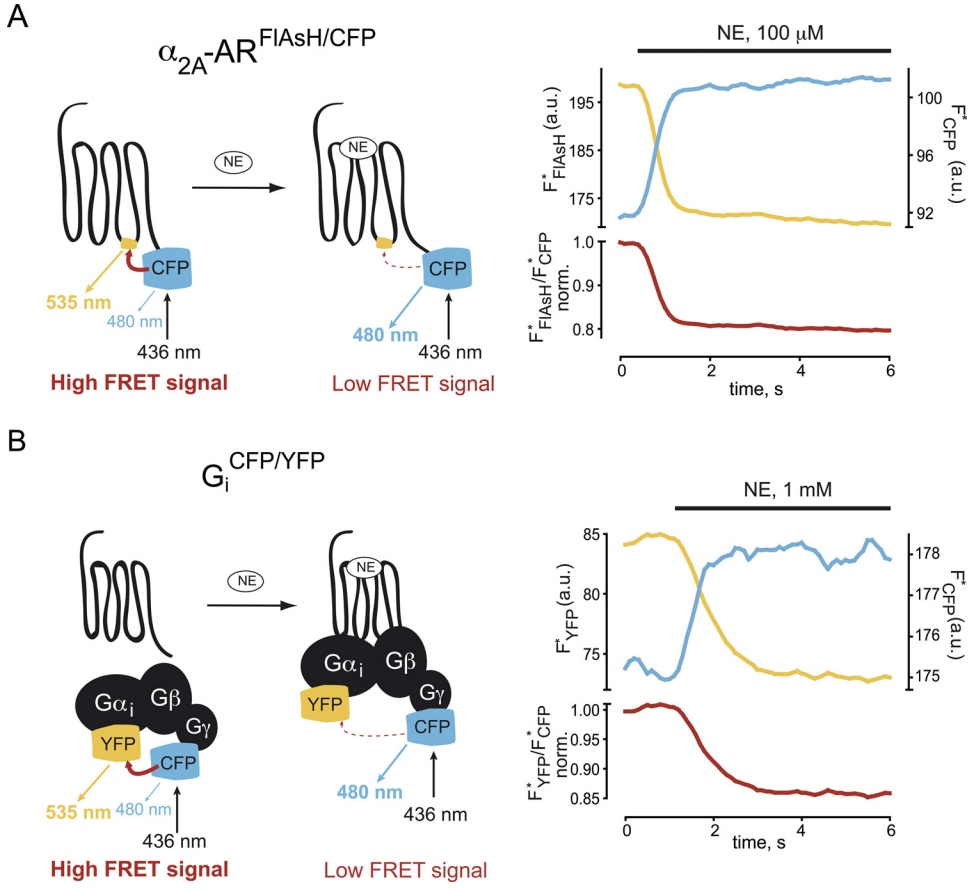

Fig. 1. Schematic model of α_{2A}-AR$^{FlAsH/CFP}$ and $G_i^{CFP/YFP}$ sensors. A, the α_{2A}-AR$^{FlAsH/CFP}$ sensor carries the donor fluorescent protein CFP at the C terminus and the acceptor fluorophore FlAsH in the third intracellular loop (left). FRET changes between the labels were determined after superfusion with the full agonist norepinephrine (NE) in single HEK-293 cells expressing the FRET-based receptor construct (right). The simultaneous decrease in FlAsH emission (F^*_{FlAsH}) (yellow trace) and increase in CFP emission (F^*_{CFP}) (blue trace) resulted in a significant decrease of the FRET ratio (F^*_{FlAsH}/F^*_{CFP}) (red trace). B, the $G_i^{CFP/YFP}$ sensor consists of the three subunits $G\alpha_{i1}$-YFP, $G\beta_1$, and $G\gamma_2$-CFP (left). HEK-293 cells expressing the $G_i^{CFP/YFP}$ sensor showed a decrease of the FRET ratio (F^*_{YFP}/F^*_{CFP}) (red trace) in response to the norepinephrine-dependent α_{2A}-AR activation (right).

$G_i^{CFP/YFP}$ sensor (Bünemann et al., 2003) by using Effectene (QIAGEN, Hilden, Germany). The amount of cDNA used for transient transfection of the wild-type α_{2A}-AR was chosen to yield overall similar receptor expression (~2 pmol/mg), as determined through radioligand binding experiments.

FlAsH Labeling. FlAsH labeling was performed as described previously (Hoffmann et al., 2005, 2010). In brief, α_{2A}-$AR^{FlAsH/CFP}$-expressing HEK-293 cells were washed twice with phenol red-free Hanks' balanced salt solution (HBSS) containing 1 g/liter glucose (Invitrogen) and subsequently were incubated for 1 h at 37°C with 500 nM FlAsH suspended in HBSS containing 12.5 μM 1,2-ethanedithiol. To reduce nonspecific labeling, cells were washed with HBSS, incubated at 37°C for 10 min with HBSS containing 250 μM ethanedithiol, and again rinsed twice with HBSS before being used for fluorescence measurements. We showed earlier that this labeling procedure does not interfere with the kinetic properties of the labeled receptors (Hoffmann et al., 2005).

Fluorescence Measurements. FRET experiments were performed with whole cells as described previously (Vilardaga et al., 2003, 2005; Hoffmann et al., 2005; Nikolaev et al., 2006; Zürn et al., 2009; Maier-Peuschel et al., 2010; Reiner et al., 2010). In brief, transfected cells grown on coverslips were washed with HBSS and maintained in buffer A (140 mM NaCl, 5 mM KCl, 2 mM $CaCl_2$, 1 mM $MgCl_2$, and 10 mM HEPES, pH 7.3) at room temperature. Coverslips were mounted on an Attofluor holder (Invitrogen) and placed on a Zeiss inverted microscope (Axiovert 135; Carl Zeiss GmbH, Jena, Germany) equipped with an oil-immersion, 100× objective and a dual-emission photometric system (TILL Photonics, Gräfelfing, Germany). Samples were excited with light from a polychrome IV system (TILL Photonics). To minimize photobleaching and to enable fast temporal resolution, the illumination and recording times were set to 14 to 40 ms and 20 to 100 ms, respectively. FRET was monitored as the YFP/CFP or FlAsH/CFP emission ratio, F_{535}/F_{480}, where F_{535} and F_{480} are the emission intensities at 535 ± 15 nm and 480 ± 20 nm (beam-splitter, long wave pass dichroic, 505 nm), respectively, upon excitation at 436 ± 10 nm (beam-splitter, long wave pass dichroic, 460 nm). Special care was taken to ensure similar fluorescence levels and distributions in the examined cells. The emission ratio was corrected with respect to the spillover of CFP fluorescence into the 535-nm channel (spillover of FlAsH and YFP fluorescence into the 480-nm channel was negligible), to yield a corrected ratio of F^*_{535}/F^*_{480}. The FlAsH (or YFP) emission upon excitation at 480 nm was recorded for each experiment, for subtraction of direct excitation from the corrected ratio. For determination of agonist-induced changes in FRET, cells were continuously superfused with buffer A, and single concentrations of norepinephrine were applied by using a computer-assisted, solenoid valve-controlled, rapid superfusion device (ALA-VM8; ALA Scientific Instruments, Westbury, NY) (solution exchange, 5–10 ms). Signals detected with avalanche photodiodes were digitized by using an analog-to-digital converter (Digidata 1322A; Molecular Devices, Sunnyvale, CA) and were stored on a personal computer by using Clampex 8.1 software (Molecular Devices). The agonist-induced decrease in the FRET ratio was fitted to the equation $A(t) = A_0 - A_1 \times e^{-t/\tau}$, where τ is the time constant (in milliseconds) and A is the amplitude of the signal.

Results

To investigate the effects of different concentrations of the full agonist norepinephrine on the speed and extent of α_{2A}-AR activation in real time, we used a FRET approach, taking advantage of the fully functional α_{2A}-$AR^{FlAsH/CFP}$ FRET sensor (Fig. 1A) (Hoffmann et al., 2005; Nikolaev et al., 2006). HEK-293 cells expressing the receptor construct were labeled with FlAsH, and single cells were monitored under a microscope for CFP and FlAsH fluorescence, as described under *Materials and Methods*. To detect changes in FRET with very high temporal resolution, we illuminated single cells with 14-ms pulses, with a frequency of 50 Hz, at 436 nm. In agreement with earlier data, superfusion with saturating concentrations of norepinephrine (1 mM) resulted in a rapid decrease in the FRET signal ($\Delta F^*_{FlAsH}/F^*_{CFP}$), because of the simultaneous increase in CFP fluorescence and decrease in FlAsH fluorescence (Fig. 1A, right). This FRET change reveals the full agonist-induced receptor activation and typically occurs on a millisecond time scale (Vilardaga et al., 2003). The maximal FRET response was high ($\Delta F^*_{FlAsH}/F^*_{CFP}$ of ~20%); therefore, superfusion of cells even with low concentrations of norepinephrine produced FRET responses with high signal/noise ratios. Figure 2A shows that stimulation with increasing concentrations of the agonist (norepinephrine at 1 μM to 1 mM) led to correspondingly increasing FRET signals (as a reference for full receptor activation for each experiment, the response was normalized to the effects of 1 mM norepinephrine at times of >2 s). The time to the half-maximal FRET response was variable and depended on the degree of receptor activation, with a saturation value for the rate constant of ~60 ms, which was achieved at high agonist concentrations (Fig. 2B).

Because the FRET-based approach applied here represents a unique tool to monitor receptor conformational changes in real time, we were able to determine the speed and extent of agonist-induced receptor activation every 20 ms. By using those FRET data, we established a pool of time-dependent concentration-response curves (a selection is shown in Fig. 3), which show EC_{50} values (i.e., effective norepinephrine concentrations evoking 50% of the maximal response) that clearly moved to the left over time until the steady state was achieved (>2 s) (Table 1). Similar to the potency, the efficacy of norepinephrine in eliciting α_{2A}-$AR^{FlAsH/CFP}$ activation increased in a time-dependent manner and then reached a saturation value (which was set to 100%).

To analyze in real time the ability of increasing concentrations of norepinephrine to produce a downstream intracellular response after α_{2A}-AR stimulation, we analyzed the kinetics and the amplitude of G_i activation in single intact cells. For this purpose, we transfected HEK-293 cells expressing the α_{2A}-AR with the well characterized $G_i^{CFP/YFP}$ sensor that consists of the three subunits $G\alpha_{i1}^{YFP}$, $G\beta_1$, and $G\gamma_2^{CFP}$ (Fig. 1B) (Bünemann et al., 2003). As shown previously, stimulation with saturating concentrations of norepinephrine triggers a robust FRET decrease ($\Delta F^*_{YFP}/F^*_{CFP}$), which is significantly slower than the maximal speed of receptor activation (Fig. 1B, right). Figure 4 represents the time-resolved FRET changes of G_i activation induced by norepinephrine concentrations ranging from 1 nM to 1 mM. For each experiment, the FRET change was normalized to the maximal effect achieved with saturating concentrations of norepinephrine. In agreement with data published previously (Bünemann et al., 2003), the amplitude of G_i activation achieved maximal values only at higher agonist concentrations (Fig. 4A). Likewise, the speed of G_i activation increased with increasing concentrations of norepinephrine, reaching the minimal value of ~600 ms at saturating concentrations of the agonist (Fig. 4B). To investigate how the potency and efficacy of norepinephrine in triggering G_i activation change under nonequilibrium conditions, we developed a series of concentration-response curves for G_i activation, starting with the FRET data recorded 100 ms after agonist superfusion

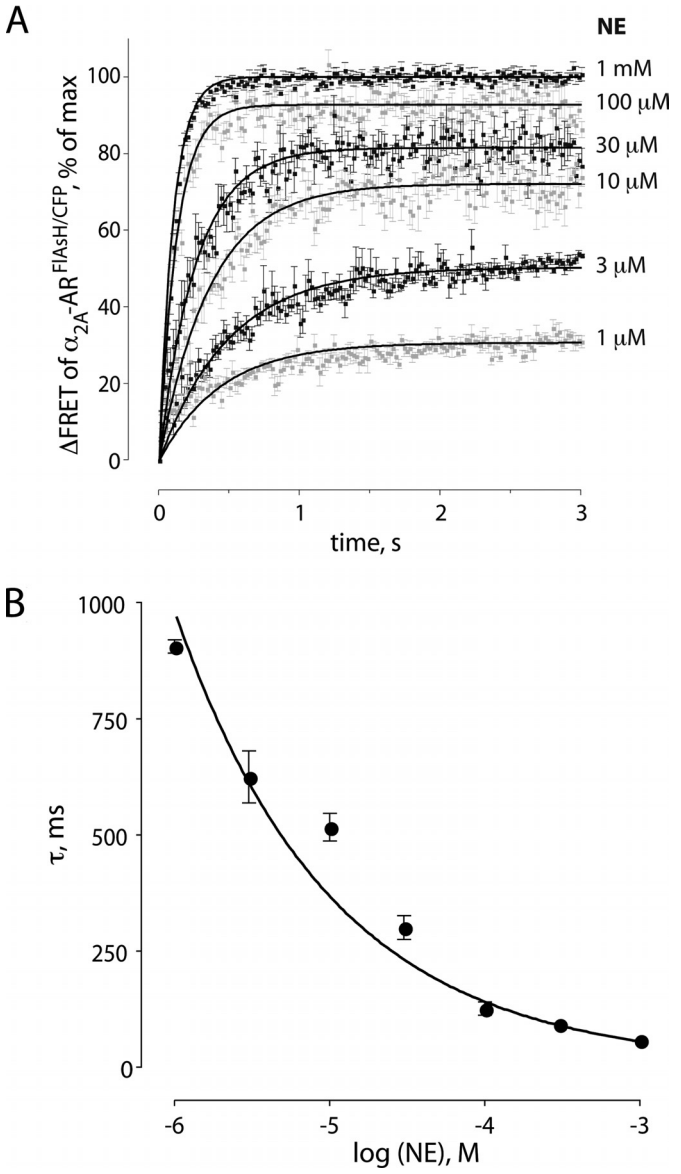

Fig. 2. Kinetics of α_{2A}-AR activation. Cells expressing the α_{2A}-AR$^{FlAsH/CFP}$ sensor were superfused with different norepinephrine (NE) concentrations. The fluorescence emissions F^*_{FlAsH} and F^*_{CFP} were recorded every 20 ms. A, relationship between norepinephrine concentrations and FRET signal amplitudes. The FRET changes were calculated as percentages of the change induced by norepinephrine at 1 mM, which was assayed in each individual experiment as a reference. B, activation time constants plotted as a function of norepinephrine concentration. Values were obtained by fitting the kinetic recordings to a monoexponential equation. For each norepinephrine concentration, data are mean ± S.E. values for 6 to 10 independent cells.

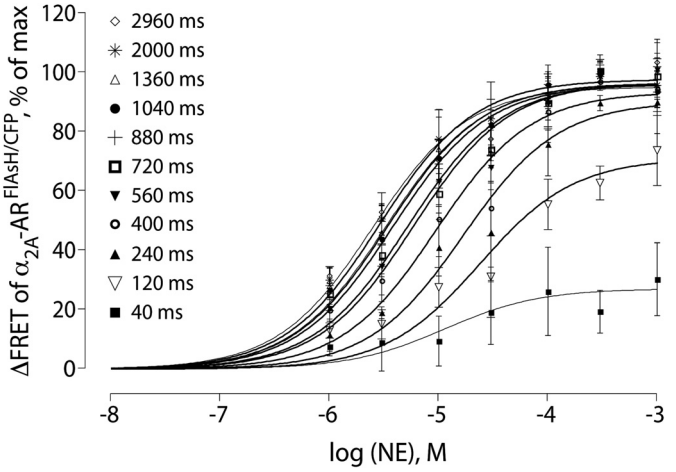

Fig. 3. Concentration-response curves for α_{2A}-AR activation under nonequilibrium conditions and at steady state. The values corresponding to the FRET amplitudes that were recorded every 20 ms until the steady state was achieved were fitted with a sigmoidal concentration-response model, which generated 150 curves. For simplification of the graph, only a selection of curves is shown; the corresponding EC_{50} values are presented in Table 1. NE, norepinephrine.

TABLE 1
Time-dependent norepinephrine potency of α_{2A}-AR$^{FlAsH/CFP}$ activation

Time	EC_{50} (95% CI)
	μM
40 ms	26.0 (13.9–50.2)
120 ms	24.5 (16.4–34.6)
240 ms	16.2 (12.4–22.7)
400 ms	9.45 (6.71–13.4)
560 ms	5.94 (4.67–7.52)
720 ms	5.22 (4.27–6.39)
880 ms	5.05 (3.19–4.53)
1040 ms	3.41 (2.75–4.24)
1360 ms	3.34 (2.59–4.14)
2000 ms	2.51 (1.99–3.08)
2960 ms	2.55 (1.99–3.12)

CI, confidence interval.

and proceeding every 100 ms until the steady state was reached. As shown in Fig. 5, both the potency and the efficacy of norepinephrine at the G-protein level depended strongly on time and reached the maximal values only under equilibrium conditions (times of >10 s). The changes in potency were best seen in the decreases in the EC_{50} values presented in Table 2.

A comparison of the time-dependent, norepinephrine-mediated effects at the α_{2A}-AR and G_i-protein levels is summarized in Fig. 6. As shown, the efficacy of norepinephrine at the receptor level reached its maximum with an apparent half-life of 58 ± 3 ms (Fig. 6A), whereas the E_{max} values at the G_i-protein level followed two-phase kinetics, with a faster component and a slower component (half-lives of 128 ± 60 ms and 658 ± 40 ms, respectively). Figure 6B, top, shows the time-dependent potency of norepinephrine at the receptor level. The EC_{50} values decreased with a half-life of 330 ± 11 ms, starting at ~26 μM (40 ms after norepinephrine superfusion) and reaching ~2 μM at steady state. As depicted in Fig. 6B, bottom, the EC_{50} values relative to G_i activation also decreased in a time-dependent manner but reached the steady state with a half-life of 2520 ± 168 ms. The potency of the full agonist norepinephrine in eliciting G_i activation started at ~100 nM after a 100-ms pulse of norepinephrine and increased exponentially until equilibrium was achieved. In the latter condition, the EC_{50} value was ~10 nM. The relationship between the potency of norepinephrine at the receptor and G-protein levels is presented in Fig. 6C, which indicates a large time-dependent amplification of the agonist-induced signal at the α_{2A}-AR.

Discussion

Classic receptor theory is largely based on in vitro measurements in which the receptor is exposed to a constant concentration of ligand under steady-state conditions (Clark,

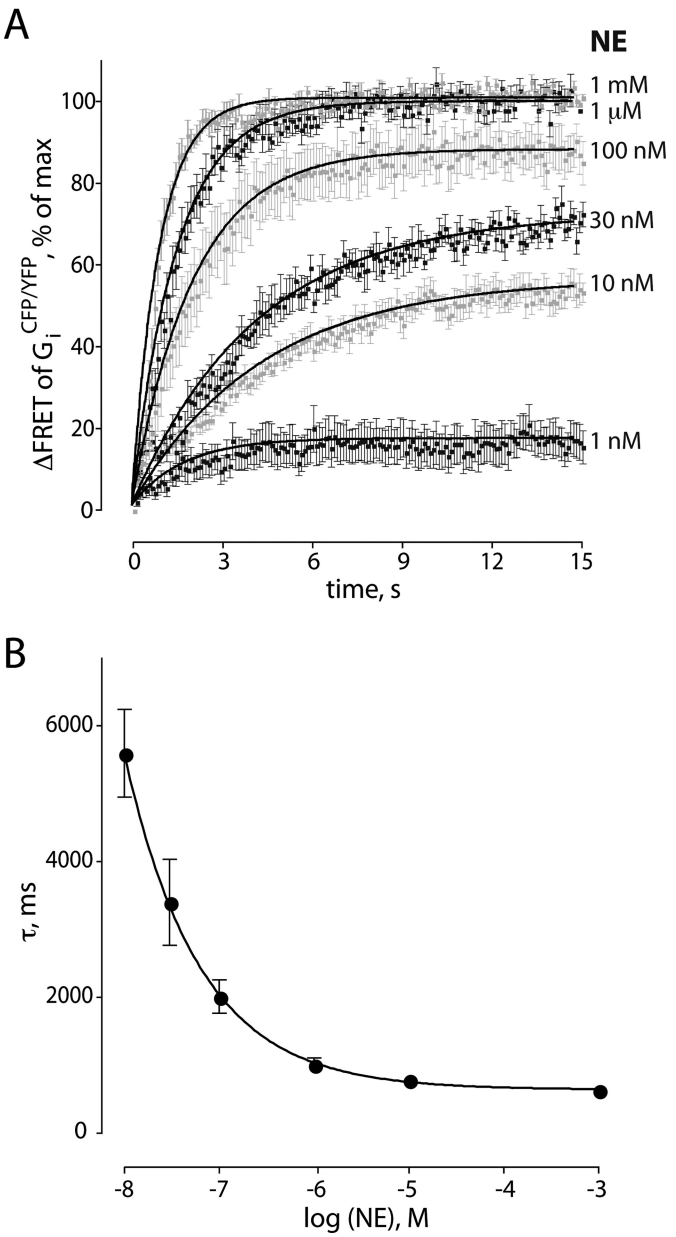

Fig. 4. Kinetics of G_i activation. Single HEK-293 cells expressing the α_{2A}-AR and the trimeric $G_i^{CFP/YFP}$ sensor were superfused with different norepinephrine (NE) concentrations. The fluorescence emissions were recorded every 100 ms. A, relationship between increasing concentrations of norepinephrine and FRET signal amplitudes. Similar to the data depicted in Fig. 2A, the FRET changes were calculated as percentages of the maximal response triggered by norepinephrine at 1 mM at equilibrium, which was assayed in each individual experiment as a reference. B, activation time constants plotted as a function of norepinephrine concentration. Values were obtained by fitting the kinetic recordings to a monoexponential equation. At saturating concentrations of norepinephrine, the speed of receptor-mediated G-protein activation was ~600 ms. For each norepinephrine concentration, data are mean ± S.E. values for 8 to 14 independent cells.

1933; Molinoff et al., 1981; Weiland and Molinoff, 1981; Black et al., 1985; Kenakin, 2002). Because a failure to attain equilibrium would lead to underestimation of ligand binding and receptor activation ability, such studies usually require long incubation times (Hulme and Trevethick, 2010). Both the theory and experimental data on the kinetics of ligand binding to receptors indicate that these processes depend on ligand concentrations (e.g., Hulme and Trevethick, 2010).

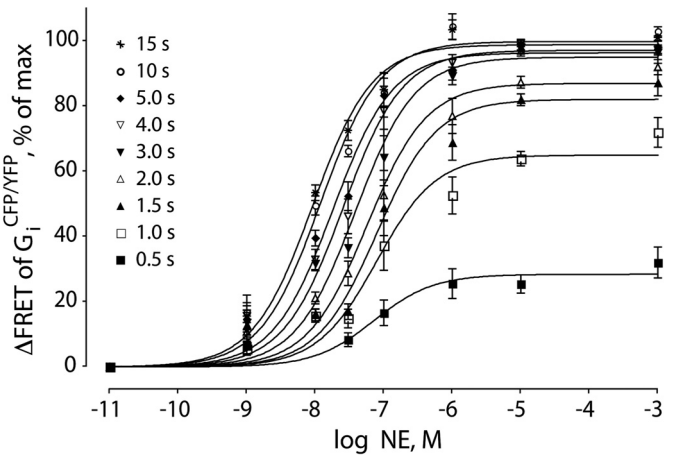

Fig. 5. Concentration-response curves for G_i activation under nonequilibrium conditions and at steady state. The values corresponding to the FRET amplitudes that were recorded every 100 ms until the steady state was reached (Fig. 4) were fitted with a sigmoidal concentration-response model and plotted as a function of norepinephrine (NE) concentration. A selection of the most significant curves is shown here, and the corresponding EC_{50} values are presented in Table 2.

TABLE 2
Time-dependent norepinephrine potency of α_{2A}-AR-mediated $G_i^{CFP/YFP}$ activation

Time	EC_{50} (95% CI)
	nM
0.5 s	103 (23.4–451)
1.0 s	77.0 (24.6–281)
1.5 s	73.2 (28.9–221)
2.0 s	59.8 (31.6–153)
3.0 s	45.3 (25.4–102)
4.0 s	25.9 (13.8–52.8)
5.0 s	20.2 (9.82–39.6)
10 s	10.1 (5.23–17.5)
15 s	9.10 (3.01–13.2)

CI, confidence interval.

These assay conditions only poorly mimic the concentrations and duration of exposure that the agonist exerts against its target in an in vivo setting. In fact, under physiological conditions (i.e., in response to nerve activity), stimulation of α_{2A}-ARs may be very short-lived but in response to high agonist concentrations. For example, it has been estimated that, in neurovascular junctions, norepinephrine concentrations might be in excess of 100 μM but for times as short as 100 ms (Bevan et al., 1984, 1987). These short stimulation pulses with high norepinephrine concentrations result from the rapid release of norepinephrine from vesicles, where its concentrations can exceed several hundred millimolar, followed by rapid reuptake (Philippu and Matthaei, 1988). To date, however, no techniques have been available for assessment of ligand binding with sufficient speed or assessment of the resultant receptor activation in real time, with the exception of the ion channel receptors, for which many kinetic experiments have been performed and theories developed (notably by Colquhoun, 2007).

To study the characteristics and kinetics of GPCR activation in a more native environment, we developed a FRET-based approach, which enables the detection of the fast activation of the receptors and their cognate G-proteins in intact cells (Lohse et al., 2008a). Here, taking advantage of those FRET-based sensors, we were able to monitor nonequilib-

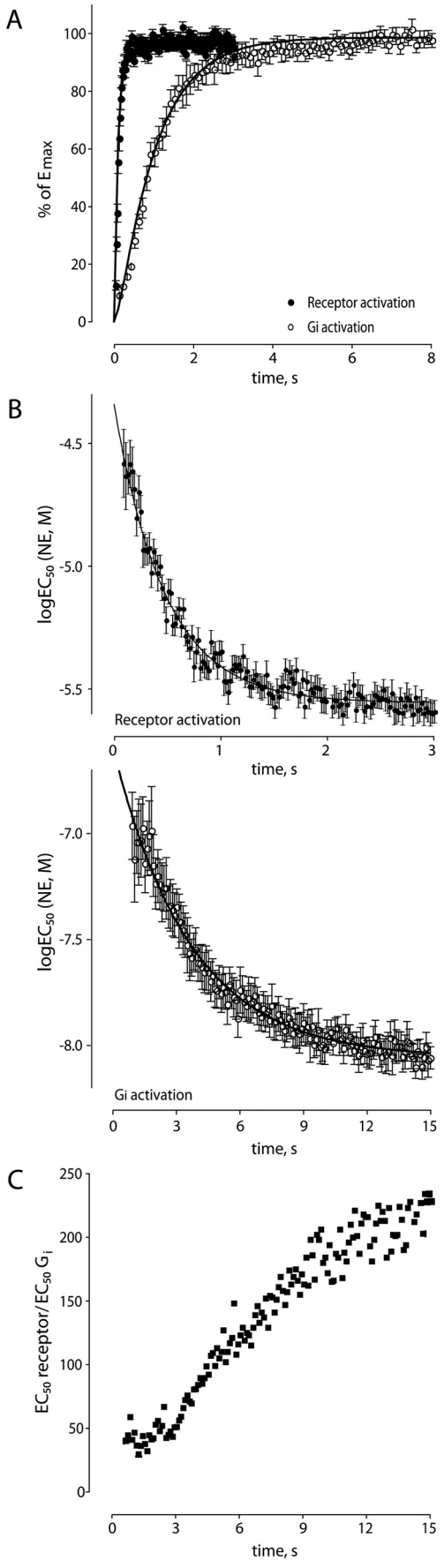

rium α_{2A}-AR function in living HEK-293 cells. The results of the time-resolved analysis of the norepinephrine-induced FRET signals recorded from single HEK-293 cells expressing the α_{2A}-AR$^{FlAsh/CFP}$ sensor are in agreement with those of earlier studies (Vilardaga et al., 2003, 2005; Hoffmann et al., 2005). First, they confirm that the extent of the FRET change is proportional to the superfused concentration of agonist, with saturating concentrations of norepinephrine triggering the maximal FRET decrease (Fig. 2A). Next, they support the notion that the speed of receptor activation depends strongly on agonist concentrations, with higher concentrations of norepinephrine triggering FRET changes more rapidly until a saturation value of ~60 ms is reached; this value presumably represents the upper limit of the true activation time of the α_{2A}-AR (Fig. 2B).

The large FRET responses and the high signal/noise ratios characterizing the α_{2A}-AR$^{FlAsh/CFP}$ sensor allowed us to monitor the agonist-dependent receptor activation with very high temporal resolution, recording the fluorescence emissions of the donor and acceptor fluorophores every 20 ms. Therefore, we were able to establish a pool of concentration-response curves under nonequilibrium conditions (Fig. 3). As expected, the efficacy of norepinephrine in eliciting α_{2A}-AR$^{FlAsH/CFP}$ activation increased in a time-dependent manner and reached its maximum with an apparent half-life of ~60 ms (Fig. 6A). As presented in Fig. 6B, top, the corresponding EC_{50} values decreased in an exponential manner, reaching ~2 μM at steady state. The equilibrium EC_{50} value of 2 μM is high, compared with potencies determined in other types of functional experiments, but it is similar to the affinity of the low-affinity state of the α_{2A}-AR, which we determined previously by performing radioligand binding experiments with cell membranes (Vilardaga et al., 2003; Nikolaev et al., 2006). It most likely represents the true affinity of the receptor in intact cells (i.e., in the non–G-protein-bound state). These observations correlate well with the apparent lack of a "receptor reserve" noted when receptor activation was monitored in intact cells.

In the GPCR signaling pathway, the interaction of an agonist-activated receptor with the cognate G-protein results in activation of the G-protein. To evaluate α_{2A}-AR activation through a receptor-mediated downstream biological response, we took advantage of a $G_i^{CFP/YFP}$ sensor, which allows direct, real-time measurement of G_i activation. The $G_i^{CFP/YFP}$ sensor gives rise to FRET responses that show relatively high signal/noise ratios, which allow the recording of FRET values every 100 ms. As expected, the amplitude of the FRET changes depended on agonist concentrations, and the time courses of G_i activation reached maximal values only at high norepinephrine concentrations (Fig. 4). The ~10-fold slower speed of G_i activation, compared with receptor

Fig. 6. Potency and efficacy of norepinephrine (NE)-dependent α_{2A}-AR activation as a function of time. A, the E_{max} values resulting from α_{2A}-AR$^{FlAsH/CFP}$ activation were fitted with a monoexponential kinetic model (half-life of ~60 ms), whereas the E_{max} values characterizing $G_i^{CFP/YFP}$ activation followed two-phase exponential kinetics (half-lives of ~130 ms and ~660 ms). B, the calculated $logEC_{50}$ values resulting from analysis of the concentration-response curves for α_{2A}-AR$^{FlAsH/CFP}$ or $G_i^{CFP/YFP}$ activation were fitted with one-phase exponential decay models and plotted as a function of time. C, the relationship between the EC_{50} values of norepinephrine required for receptor and G-protein activation was calculated as the ratio of the EC_{50} values resulting from the analysis of the concentration-response curves depicted in Figs. 3 and 5.

activation, is in agreement with earlier data that suggest that G-protein activation is the rate-limiting step in the activation of the signaling cascade (Hein et al., 2005, 2006). The development of nonequilibrium concentration-response curves by using the FRET data on G_i activation confirms that, with our FRET-based approach in intact cells, we can experimentally reproduce the classic receptor theory predictions. As depicted in Fig. 6A, the efficacy of norepinephrine in activating the cognate G_i-protein increased until equilibrium was achieved. Here, in contrast to the receptor activation kinetics, the E_{max} values followed two-phase kinetics, which agree very well with the notion that, after rapid G-protein recruitment to the activated receptor, a slow step (probably GDP release from the G-protein) limits the speed of G-protein activation, which makes it the time-limiting step of the signaling cascade (Hein et al., 2006). As shown in Fig. 6B, bottom, the EC_{50} values for G_i activation decreased in a time-dependent manner and reached the steady state ~8 times more slowly than shown for activation of the receptor. The equilibrium EC_{50} value of the full agonist norepinephrine in eliciting G_i activation was ~10 nM, in accordance with a high degree of receptor reserve existing in our transfected cell system and corresponding to the presence of a large receptor reserve identified in electrophysiological studies with transfected cells (Bünemann et al., 2001).

A comparison of the two panels in Fig. 6B reveals the differences in norepinephrine concentrations required to elicit half-maximal responses for the receptor and for G_i. As shown in Fig. 6C, these data illustrate that, over short stimulation phases, the amplification between receptors and G-proteins first becomes smaller, because receptors initially are activated faster than G_i, but then continues to increase until it achieves 2.5 orders of magnitude. This large amplification demonstrates a large receptor reserve, which means that only a fraction of the receptors available on the cell membrane need to be activated to generate a maximal downstream signaling effect (Nickerson, 1956; Ariens et al., 1960). This concept has been much discussed on the basis of various types of analyses of neurotransmitter release experiments (Agneter et al., 1993, 1997). Many biological systems involving α_{2A}-ARs have been reported to display large receptor reserves, including presynaptic control of neurotransmitter release in various brain regions (Adler et al., 1987), prejunctional receptors at the vas deferens (Sallés et al., 1994), receptors on human platelets (Lenox et al., 1985), receptors controlling venous (but not arterial) tone (Ruffolo, 1986), and receptors controlling behavioral and physiological responses (Durcan et al., 1994). Our data now show that the signal amplification underlying the receptor reserve is time-dependent and increases, in our case, by almost 1 order of magnitude over a period of ~15 s.

In conclusion, the high temporal resolution achieved with our FRET-based technology was successfully applied to monitor norepinephrine-mediated effects on α_{2A}-AR activation and signaling in real time. Taken together, our experimental findings reflect well the physiological synaptic events and resemble the theoretical predictions of classic receptor theory, which postulate that, under nonequilibrium conditions, higher agonist concentrations are required to achieve receptor binding and activation (Convents et al., 1987; Severne et al., 1987). Over stimulation times of less than 1 s, agonist potency and efficacy at the receptor increase, followed by similar increases at the level of G_i that occur over a few seconds. Therefore, receptor-mediated signaling and signal amplification are highly dependent on stimulation times. This adds another level of complexity to agonist effects at G-protein-coupled receptors.

Authorship Contributions

Participated in research design: Ambrosio and Lohse.
Conducted experiments: Ambrosio.
Performed data analysis: Ambrosio.
Wrote or contributed to the writing of the manuscript: Ambrosio and Lohse.

References

Adler CH, Meller E, and Goldstein M (1987) Receptor reserve at the alpha-2 adrenergic receptor in the rat cerebral cortex. *J Pharmacol Exp Ther* **240:**508–515.
Agneter E, Drobny H, and Singer EA (1993) Central α_2-autoreceptors: agonist dissociation constants and recovery after irreversible inactivation. *Br J Pharmacol* **108:**370–375.
Agneter E, Singer EA, Sauermann W, and Feuerstein TJ (1997) The slope parameter of concentration-response curves used as a touchstone for the existence of spare receptors. *Naunyn Schmiedebergs Arch Pharmacol* **356:**283–292.
Ariens EJ, van Rossum J, and Koopman PC (1960) Receptor reserve and threshold phenomena. I. Theory and experiments with autonomic drugs tested on isolated organs. *Arch Int Pharmacodyn Ther* **127:**459–478.
Bevan JA, Laher I, and Rowan R (1987) Some implications of the high intrasynaptic norepinephrine concentrations in resistance arteries. *Blood Vessels* **24:**137–140.
Bevan JA, Tayo FM, Rowan RA, and Bevan RD (1984) Presynaptic alpha-receptor control of adrenergic transmitter release in blood vessels. *Fed Proc* **43:**1365–1370.
Black JW, Leff P, Shankley NP, and Wood J (1985) An operational model of pharmacological agonism: the effect of E/[A] curve shape on agonist dissociation constant estimation. *Br J Pharmacol* **84:**561–571.
Bünemann M, Bücheler MM, Philipp M, Lohse MJ, and Hein L (2001) Activation and deactivation kinetics of α_{2A}- and α_{2C}-adrenergic receptor-activated G protein-activated inwardly rectifying K^+ channel currents. *J Biol Chem* **276:**47512–47517.
Bünemann M, Frank M, and Lohse MJ (2003) G_i protein activation in intact cells involves subunit rearrangement rather than dissociation. *Proc Natl Acad Sci USA* **100:**16077–16082.
Clark AJ (1933) *The Mode of Action of Drugs on Cells*, E Arnold Co., London.
Colquhoun D (2007) What have we learned from single ion channels? *J Physiol* **581**:425–427.
Convents A, De Backer JP, Convents D, and Vauquelin G (1987) Tight agonist binding may prevent the correct interpretation of agonist competition binding curves for α_2-adrenergic receptors. *Mol Pharmacol* **32:**65–72.
Durcan MJ, Morgan PF, Van Etten ML, and Linnoila M (1994) Covariation of α_2-adrenoceptor density and function following irreversible antagonism with EEDQ. *Br J Pharmacol* **112:**855–860.
Hein L (2006) Adrenoceptors and signal transduction in neurons. *Cell Tissue Res* **326:**541–551.
Hein P, Frank M, Hoffmann C, Lohse MJ, and Bünemann M (2005) Dynamics of receptor/G protein coupling in living cells. *EMBO J* **24:**4106–4114.
Hein P, Rochais F, Hoffmann C, Dorsch S, Nikolaev VO, Engelhardt S, Berlot CH, Lohse MJ, and Bünemann M (2006) G_s activation is time-limiting in initiating receptor-mediated signaling. *J Biol Chem* **281:**33345–33351.
Hoffmann C, Gaietta G, Bünemann M, Adams SR, Oberdorff-Maass S, Behr B, Vilardaga JP, Tsien RY, Ellisman MH, and Lohse MJ (2005) A FlAsH-based FRET approach to determine G protein-coupled receptor activation in living cells. *Nat Methods* **2:**171–176.
Hoffmann C, Gaietta G, Zürn A, Adams SR, Terrillon S, Ellisman MH, Tsien RY, and Lohse MJ (2010) Fluorescent labeling of tetracysteine-tagged proteins in intact cells. *Nat Protoc* **5:**1666–1677.
Hulme EC and Trevethick MA (2010) Ligand binding assays at equilibrium: validation and interpretation. *Br J Pharmacol* **161:**1219–1237.
Jensen JB, Lyssand JS, Hague C, and Hille B (2009) Fluorescence changes reveal kinetic steps of muscarinic receptor-mediated modulation of phosphoinositides and Kv7.2/7.3 K^+ channels. *J Gen Physiol* **133:**347–359.
Kenakin T (2002) Efficacy at G-protein-coupled receptors. *Nat Rev Drug Discov* **1:**103–110.
Lefkowitz RJ (2000) The superfamily of heptahelical receptors. *Nat Cell Biol* **2:**E133–E136.
Lenox RH, Ellis J, Van Riper D, and Ehrlich YH (1985) Alpha 2-adrenergic receptor-mediated regulation of adenylate cyclase in the intact human platelet: evidence for a receptor reserve. *Mol Pharmacol* **27:**1–9.
Lohse MJ, Hein P, Hoffmann C, Nikolaev VO, Vilardaga JP, and Bünemann M (2008a) Kinetics of G-protein-coupled receptor signals in intact cells. *Br J Pharmacol* **153 (Suppl 1):**S125–S132.
Lohse MJ, Nikolaev VO, Hein P, Hoffmann C, Vilardaga JP, and Bünemann M (2008b) Optical techniques to analyze real-time activation and signaling of G-protein-coupled receptors. *Trends Pharmacol Sci* **29:**159–165.
Maier-Peuschel M, Frölich N, Dees C, Hommers LG, Hoffmann C, Nikolaev VO, and Lohse MJ (2010) A fluorescence resonance energy transfer-based M2 muscarinic receptor sensor reveals rapid kinetics of allosteric modulation. *J Biol Chem* **285:**8793–8800.
Molinoff PB, Wolfe BB, and Weiland GA (1981) Quantitative analysis of drug-

receptor interactions: II. Determination of the properties of receptor subtypes. *Life Sci* **29:**427–443.
Nickerson M (1956) Receptor occupancy and tissue response. *Nature* **178:**697–698.
Nikolaev VO, Hoffmann C, Bünemann M, Lohse MJ, and Vilardaga JP (2006) Molecular basis of partial agonism at the neurotransmitter α_{2A}-adrenergic receptor and G_i-protein heterotrimer. *J Biol Chem* **281:**24506–24511.
Park J, Kile BM, and Wightman RM (2009) In vivo voltammetric monitoring of norepinephrine release in the rat ventral bed nucleus of the stria terminalis and anteroventral thalamic nucleus. *Eur J Neurosci* **30:**2121–2133.
Park J, Takmakov P, and Wightman RM (2011) In vivo comparison of norepinephrine and dopamine release in rat brain by simultaneous measurements with fast-scan cyclic voltammetry. *J Neurochem* **119:**932–944.
Philipp M and Hein L (2004) Adrenergic receptor knockout mice: distinct functions of 9 receptor subtypes. *Pharmacol Ther* **101:**65–74.
Philippu A and Matthaei H (1988) Transport and storage of catecholamines in vesicles. *Handb Exp Pharmacol* **90:**1–42.
Reiner S, Ambrosio M, Hoffmann C, and Lohse MJ. (2010) Differential signaling of the endogenous agonists at the β_2-adrenergic receptor. *J Biol Chem* **285:**36188–36198.
Ruffolo RR Jr (1986) Spare α adrenoceptors in the peripheral circulation: excitation-contraction coupling. *Fed Proc* **45:**2341–2346.
Sallés J, Giraldo J, and Badia A (1994) Analysis of agonism at functional prejunctional α_2-adrenoceptors of rat vas deferens using operational and null approaches. *Eur J Pharmacol* **258:**229–238.
Severne Y, Ijzerman A, Nerme V, Timmerman H, and Vauquelin G (1987) Shallow agonist competition binding curves for β-adrenergic receptors: the role of tight agonist binding. *Mol Pharmacol* **31:**69–73.
Vilardaga JP, Bünemann M, Krasel C, Castro M, and Lohse MJ (2003) Measurement of the millisecond activation switch of G protein-coupled receptors in living cells. *Nat Biotechnol* **21:**807–812.
Vilardaga JP, Steinmeyer R, Harms GS, and Lohse MJ (2005) Molecular basis of inverse agonism in a G protein-coupled receptor. *Nat Chem Biol* **1:**25–28.
Weiland GA and Molinoff PB (1981) Quantitative analysis of drug-receptor interactions. I. Determination of kinetic and equilibrium properties. *Life Sci* **29:**313–330.
Zürn A, Zabel U, Vilardaga JP, Schindelin H, Lohse MJ, and Hoffmann C (2009) Fluorescence resonance energy transfer analysis of α_{2A}-adrenergic receptor activation reveals distinct agonist-specific conformational changes. *Mol Pharmacol* **75:**534–541.

Address correspondence to: Dr. M. J. Lohse, Institute of Pharmacology and Toxicology, Versbacher Straße 9, D-97078 Würzburg, Germany. E-mail: lohse@toxi.uni-wuerzburg.de